Joint Data/Channel Estimation for Frequency Selective (Time-Varying) Multi-path Channels with Antenna Arrays

Serdar Özen and Michael D. Zoltowski

School of Electrical & Computer Engineering
Purdue University
West Lafayette, IN 47907-1285
email: {ozen, mikedz}@ecn.purdue.edu

Abstract — **A joint data and channel estimation/tracking algorithm is presented for the time varying frequency selective multi-path fading channel. An in-depth formulation of time varying frequency selective channel structure is developed for a receiver employing multiple antennae where the formulation of the channel model enables channel tap delays a fraction of the symbol period. Moreover the Doppler frequency shifts are embedded in the formulation. State-space formulation developed for the time varying channel leads to the recursive least square (RLS) channel estimator, and a Kalman channel state tracker. The data estimation is accomplished by using the Viterbi algorithm (MLSE-VA). The MLSE-VA used here is the Per-Branch-Processing Viterbi Algorithm [4] (PBP-VA) which enables the updated channel estimates to be used in the metric computations of the data sequence estimation process. BER performance of the receiver will be presented for different estimators.**

I. INTRODUCTION

The problem of data detection in a wireless communication system where the channel state information is not fully known by the receiver, and the channel is assumed to be a rapidly time-varying, frequency selective Rayleigh fading channel, has been studied recently [2, 4]. The channel estimation/tracking is accomplished by using RLS and Kalman filtering algorithms, while the data sequence estimation is accomplished by the PBP MLSE-VA. In [2] problem formulation does not include the Doppler shift in frequency which is due to the movements of the communicating mobile units and/or the movements of the environment. Even though [4] includes the Doppler shifts in the formulation, receivers employing multiple antennae and the possibility of channels taps being a fraction of the symbol duration have not been considered in the channel model structure. In this paper we extend the formulations developed in [2, 4] to handle the case when the time varying channel taps are a fraction of symbol duration, an antenna array is employed at the receiver, fractional sampling rate (of the symbol duration) is employed at the receiver, the receiver pre-estimates the channel state-space matrices; as opposed to readily assuming the partial channel state information is available. Actual Doppler frequency shifts were assumed to be available in [4].

II. SIGNAL MODEL FOR TIME-VARYING MULTI-PATH CHANNELS

The base-band transmitted signal waveform depicted in Figure 1 is represented by

$$s(t) = \sum_{k=1}^{N_b} d_k p(t - kT) \qquad (1)$$

where $\{d_k \in A \equiv \{\alpha_1, \ldots, \alpha_M\} \subset \mathbf{C}^1\}$ is the transmitted data sequence, of burst length N_b, which is a discrete M-ary sequence taking values on the generally complex M-ary alphabet A, which also constitutes the two dimensional employed modulation constellation. $p(t)$ is the transmitter pulse shaping filter. The channel impulse response, or the *input delay-*
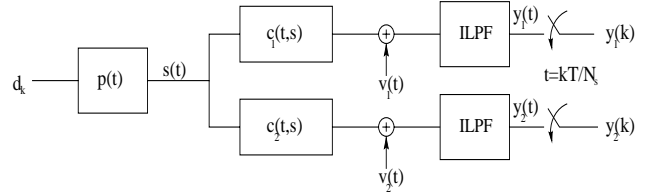

Fig. 1: Simplified system model of time-varying frequency selective fading channel model with $N_A = 2$.

spread function [1], for each antenna are denoted by $c_i(t, \tau)$ and given by

$$c_i(t, \tau) = \sum_{l=0}^{\tau_d} c_{i,l}(t)\delta(\tau - \tau_l) = \sum_{l=0}^{\tau_d} c_{i,l}(t)\delta(\tau - lT_s) \qquad (2)$$

where we assumed channel tap spacing is equal to the sampling interval, that is $\tau_l = lT_s = lT/N_s$, and $c_{i,l}(t)$ denote the complex time-varying coefficients of the channel impulse response for the ith antenna ($1 \leq i \leq N_A$). Figure II is a simplified sketch of the impulse response seen at the ith antenna at some time t_o. The range of delays, τ_d is called the *delay spread*. In the sequel the cascade of the channel impulse re-
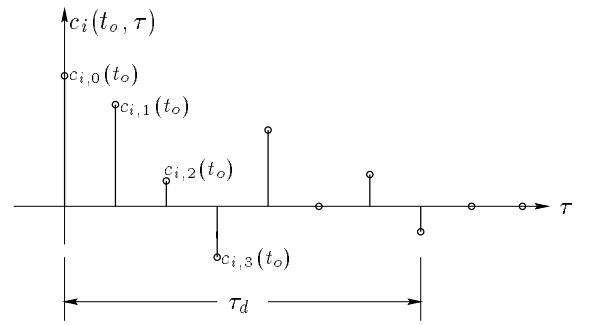

Fig. 2: Sketch of an impulse response seen at some time t_o

sponse, $c_i(t, \tau)$, with the transmitter pulse shaping filter, $p(t)$, will be denoted by $h_i(t, \tau)$, and it is defined as

$$h_i(t, \tau) = \int_{-\infty}^{\infty} c_i(t, \lambda)p(\tau - \lambda)\, d\lambda = \sum_{l=0}^{L} c_{i,l}(t)p(\tau - lT_s). \qquad (3)$$

The second equality is obtained from substituting the definition of $c_i(t, \tau)$ from Equation (2). Let $r_i(t)$ be the received

signal without the additive noise term at the ith antenna. We also assumed that the impulse response of $p(\cdot)$ is truncated to a finite length L_p such that the total length of the correlated samples is $L = \tau_d + L_p$. $r_i(t)$ can be written by

$$
\begin{aligned}
r_i(t) &= \left(\sum_{k=1}^{N_b} d_k \delta(t - kT) \right) * h_i(t, \tau) \\
&= \sum_{k=1}^{N_b} d_k h_i(t, t - kT).
\end{aligned} \tag{4}
$$

For all practical purposes it can be assumed that the transmitted signal $s(t)$ is band-limited. Although $r_i(t)$ is expanded by the Doppler spread, which is usually much smaller than the bandwidth of $s(t)$, $r_i(t)$ can be assumed to be a band-limited signal of bandwidth B Hertz. The output of the ILPF is sampled at the Nyquist rate ($T_s = \frac{1}{2B}$). After the low-pass filtering the signal $y_i(t)$ is given by

$$
y_i(t) = r_i(t) + \nu_i(t) \tag{5}
$$

where $\nu_i(t)$ is the low-pass filtered additive noise $\tilde{\nu}_i(t)$ with a power spectral density $S_{\tilde{\nu}}(f) = \tilde{N}_0$. In the sequel discrete time signals will be denoted by square brackets, and the corresponding discrete time index will denote the $T_s = T/N_s$-spaced epoch index, where T is the symbol duration and $N_s \geq 1$. After ideal low-pass filtering, $y_i[n] \equiv y_i(nT/N_s)$ is the N_s times over-sampled version of $y_i(t)$, and using (4) and (5), $y_i[n]$ can be expressed by

$$
\begin{aligned}
y_i[n] \equiv y_i(nT_s) &= \sum_{k=1}^{N_b} d_k h_i(nT_s, nT_s - kT) + \nu_i(nT_s) \\
&= \sum_{k=1}^{N_b} d_k h_i[n, n - kN_s] + \nu_i[n],
\end{aligned} \tag{6}
$$

where $\{\nu_i[n] \equiv (\nu_i^c[n] + j\nu_i^s[n]) \in \mathbf{C}^1, n \geq 1\}$ represents zero-mean independent Gaussian stationary complex white noise with variance $N_0 = 2B\tilde{N}_0$ per component [5], and $\{\nu_i[n]\}_{i=1}^{N_A}$ is independent from the data sequence $\{d_k\}$, and $\{\nu_i^c[n]\}$ and $\{\nu_i^s[n]\}$ are mutually uncorrelated. Defining

$$
a_k = \sum_n d_n \delta(k - nN_s) = \begin{cases} b_k, & \text{if } \frac{k}{N_s} \in \mathbf{Z} \\ 0, & \text{otherwise,} \end{cases} \tag{7}
$$

and defining the summation index as $m = kN_s$, we can rewrite (6) as

$$
y_i[n] = \sum_{m=1}^{N_s N_b} a_m h_i[n, n - m] + \nu_i[n], \tag{8}
$$

from Equation (3) $h_i[n, n - m]$ is given by

$$
h_i[n, n - m] = \sum_{l=0}^{L} c_{i,l}[n] p[(n - m) - l]. \tag{9}
$$

Letting $k = n - m$, the cascade of the channel impulse response, $c_i(t, \tau)$, with the transmitter pulse shaping filter, $p(t)$, can be written in discrete-time as

$$
h_i[n, k] = \sum_{l=0}^{L} c_{i,l}[n] p[k - l]. \tag{10}
$$

III. Derivation of the Fading Filter

A straightforward method to simulate a faded signal is to amplitude modulate the carrier signal with a low-pass filtered Gaussian noise source as shown in Figure III. If the Gaussian noise sources have zero-mean then this method produces a Rayleigh faded envelope [7]. In order to obtain time vary-
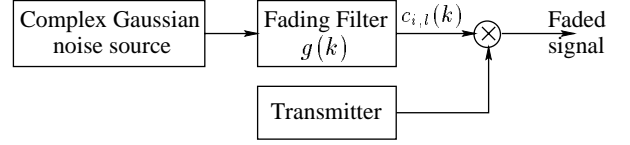

Fig. 3: Faded signal generator that uses low-pass filtered white complex Gaussian noise

ing *frequency selective fading channel* we must have a bank of these fading filters where each filter generates the corresponding fading channel tap. If we consider a receiver employing an antenna array, then we need to consider different channels for each antenna. An illustration of the antenna array case with $N_A = 2$ is provided in Figure 4, where only two ray channel per antenna (one direct path, and one delayed) has been considered for the sake of simplicity.
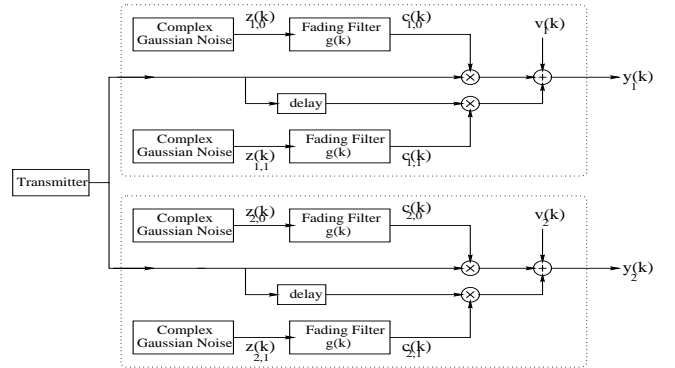

Fig. 4: Time-varying frequency selective fading channel model with $N_A = 2$ antennae, and with one direct and one delayed path for each antenna.

It is well known that a Rayleigh fading process is characterized by its power spectrum density, and its auto-correlation function. Theoretical *spectral density* of the complex envelope of the *faded* un-modulated carrier waveform is represented as [3]

$$
S(f) = \begin{cases} \dfrac{\sigma^2}{2\pi f_d \sqrt{1 - (f/f_d)^2}} & |f| < f_d \\ 0 & \text{else} \end{cases} \tag{11}
$$

where σ^2 is the rms value of the envelope of the waveform, or equivalently it is the fractional power of each lag. f_d is the maximum Doppler shift which is defined as the ratio of the vehicle speed, V, to the wavelength, λ, $f_d = V/\lambda$, and $\lambda = c/f_c$ where $c = 3 \times 10^8 m/sec$ is the speed of the light, and f_c(Hz) is the carrier frequency. The corresponding auto-correlation function of the fading process is given by [3]

$$
\Phi(\tau) = \sigma^2 J_0(2\pi f_d \tau) \tag{12}
$$

where $J_0(\cdot)$ is the zero order Bessel function of the first kind. A *fading filter* with impulse response $g(k)$ can be designed so

Tab. 1: Ratio of w_x/w_d tabulated with respect to various filter orders, and desired peak (dB) at $w = w_x$

Filter Order	Desired peak (dB) at $w = w_x$		
γ	10	15	20
2	1.0200	1.0055	1.0025
3	1.0152	1.0060	1.0017
4	1.0668	1.0401	1.0247
5	1.0668	1.0413	1.0228

Fig. 5: Theoretical and approximate spectral density (for the second order filter $G_2(s)$), and theoretical and approximate auto-correlation sequence for the channel tap coefficients.

that its output spectral density is an approximation to $S(f)$. We will use filter structures which are similar to those that were proposed in [4], but we will use a somewhat different optimization/design criterion to set their parameters. Consider

$$G_1(s) = \frac{w_x}{s + w_x}, \text{ and } G_2(s) = \frac{w_x^2}{s^2 + \frac{w_x s}{Q} + w_x^2}.$$

Then we can have fading filter continuous time transfer functions with higher orders (of order γ), $G_\gamma(s)$, that are given by

$$G_\gamma(s) = \begin{cases} G_2^{\gamma/2}(s), & \text{if } \gamma \text{ even} \\ G_1(s)G_2^{(\gamma-1)/2}(s), & \text{if } \gamma \text{ odd} \end{cases}$$

Select Q such that there is a pre-specified frequency response level at $w = w_x \text{rad/sec}$; for example for the third-order filter if $Q = \sqrt{10}$ then the magnitude of $G(\cdot)$ will have a gain of 7dB at $w = w_x$ (10dB gain from the second order filter and -3dB from the first order part making an overall gain of 7dB).

In order to find the parameters of the fading filter transfer function, $G_\gamma(s)$, we will first set the filter order γ and Q. Then defining $S(f; \epsilon)$, as an approximation to the theoretical spectral density of (11), by

$$S(f; \epsilon) = \begin{cases} \frac{\sigma^2}{2\pi f_d \sqrt{1 - (f/f_d)^2}} & |f| \leq f_d - \epsilon \\ 0 & \text{else} \end{cases} \quad (13)$$

where $\epsilon \in \mathbf{R}^+$ is a very small positive real number, which can be taken as the smallest positive number the computing platform that can handle. Then we solved the numerical optimization problem, for fixed γ, f_d and Q, $w_x = \arg\min \| S(f; \epsilon) - |G_\gamma(j2\pi f)|^2 \|$; the result of this numerical optimization gives the minimizer of the norm of the distance between the modified theoretical spectral density and the fading filter spectrum. As an example we selected the parameters $f_c = 1$GHz, $v = 90$km/h$= 25$m/sec, causing the maximum Doppler frequency shift $f_d = 83\frac{1}{3}$Hz. The table shows the ratio of w_x to w_d, for various values of Q and filter order γ.

Once the appropriate transfer function, $G_\gamma(s)$, is obtained in the s-domain, we can use the *bilinear transform* to get $G(z)$ with an ARMA(γ, γ) model, or *impulse invariance method* to get a $G(z)$ with an AR(γ) model (all pole filter) [6] . Assume that, we have an ARMA(γ, γ) model with transfer function

$$G_\gamma(z) = \frac{\sum_{k=0}^{\gamma} g_k^M z^{-k}}{1 - \sum_{k=1}^{\gamma} g_k^A z^{-k}}. \quad (14)$$

For a second order filter the corresponding output spectral density, $S_{G_2}(w) = |G_2(jw)|^2$, and the auto-correlation function are provided in comparison with the theoretical spectral density and auto-correlation sequence in Figure 5.

On the other hand, from Figure 4 we can see that the fading channel coefficients $c_{i,l}[n]$, $1 \leq i \leq N_A$, $0 \leq l \leq L$, can
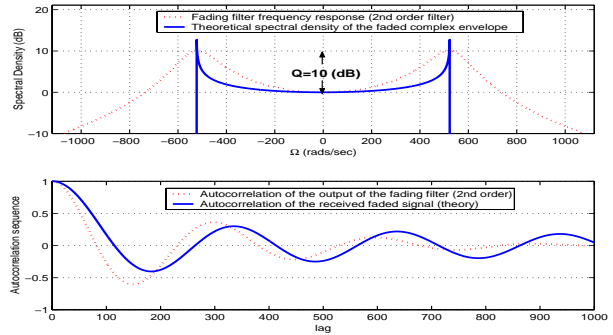
be obtained as the outputs of the fading filter, and can be written as

$$c_{i,l}[n] = g_\gamma[n] * z_{i,l}[n] \quad (15)$$

where $g_\gamma[n]$ is the impulse response of the fading filter, and $z_{i,l}[n]$ denote the complex white Gaussian noise sequence. Then substituting (15) into (10), $h_i[n, k]$ is given by

$$h_i[n, k] = \sum_{l=0}^{L} (z_{i,l}[n]p[k - l]) * g_\gamma[n]. \quad (16)$$

Defining

$$\tilde{w}_i[n, k] = \sum_{l=0}^{L} z_{i,l}[n]p[k - l], \quad (17)$$

we obtain

$$h_i[n, k] = \tilde{w}_i[n, k] * g_\gamma[n]. \quad (18)$$

Given the transfer function of the fading filter, $G_\gamma(z)$, as in (14), and using (18) the ARMA(γ, γ) representation of the discrete-time channel impulse response can be obtained as

$$h_i[n, k] = \sum_{k=1}^{\gamma} g_k^A h_i[n - m, k] + \sum_{m=0}^{\gamma} g_k^M \tilde{w}_i[n - m, k]. \quad (19)$$

IV. THE STATE-SPACE MODEL

The wireless communication system illustrated in Figure 1, leads to the state-space formulation which is compactly written as

$$\text{state equation:} \quad \mathbf{x}[k + 1] = \mathbf{A}\mathbf{x}[k] + \mathbf{B}\mathbf{W}[k + 1] \quad (20)$$
$$\text{observation equation:} \quad \mathbf{y}[k] = \mathbf{C}_k\mathbf{x}[k] + \boldsymbol{\nu}[k] \quad (21)$$

where $\mathbf{x}[k]$ is the channel state variable and defined by

$$\mathbf{x}[k] \equiv [\mathbf{H}[k]^T, \mathbf{H}[k - 1]^T, \cdots, \mathbf{H}[k - \gamma + 1]^T]^T, \quad (22)$$

$$\mathbf{H}[k] = \sum_{n=1}^{\gamma} g_n^A I_{(L+1)N_A} \mathbf{H}[k - n] + \sum_{n=0}^{\gamma} g_n^M I_{(L+1)N_A} \mathbf{w}[k - n] \quad (23)$$

where $\mathbf{H}[k] = [\mathbf{h}_1[k]^T, \mathbf{h}_2[k]^T, \cdots, \mathbf{h}_{N_A}[k]^T]^T$, and $\mathbf{h}_i[k] = [h_i[k, 0], h_i[k, 1], \cdots, h_i[k, L]]^T$. Recognizing the formulation

of the channel state vector $\mathbf{H}[k]$ in (23), the state space equation matrices $\mathbf{A}$ and $\mathbf{B}$ in Equation 20 can be written by

$$\mathbf{A} = \begin{bmatrix} g_1^A I & g_2^A I & \cdots & \cdots & g_\gamma^A I \\ I & 0 & \cdots & \cdots & 0 \\ 0 & I & 0 & \cdots & 0 \\ \vdots & 0 & \ddots & 0 & 0 \\ 0 & \cdots & 0 & I & 0 \end{bmatrix}_{(L+1)N_A\gamma \times (L+1)N_A\gamma} ,$$

$$\mathbf{B} = \begin{bmatrix} g_0^M I & g_1^M I & \cdots & g_\gamma^M I \\ 0 & 0 & \cdots & 0 \\ 0 & 0 & \cdots & 0 \\ \vdots & \vdots & \cdots & \vdots \\ 0 & 0 & \cdots & 0 \end{bmatrix}_{(L+1)N_A\gamma \times (L+1)N_A(\gamma+1)} .$$

$\mathbf{W}[k] = [\mathbf{w}[k]^T, \mathbf{w}[k-1]^T, \cdots, \mathbf{w}[k-\gamma]^T]^T$, and $\mathbf{w}[k]$ is a $(L+1)N_A$ dimensional zero mean Gaussian process, defined by $\mathbf{w}[k] = [\tilde{\mathbf{w}}_1[k]^T, \tilde{\mathbf{w}}_2[k]^T, \cdots, \tilde{\mathbf{w}}_{N_A}[k]^T]^T$ where $\tilde{\mathbf{w}}_i[k] = [\tilde{w}_i[k,0], \tilde{w}_i[k,1], \cdots, \tilde{w}_i[k,L]]^T$. The covariance matrix of $\mathbf{W}[k]$, which is defined by

$$\frac{1}{2}E\{\mathbf{W}[k]\mathbf{W}^H[l]\} = \mathbf{Q}\delta_{kl}, \tag{24}$$

will be composed of $N_A(\gamma+1)$ block diagonal matrices $\tilde{\mathbf{Q}}(i)$, and the elements of the matrix $\tilde{\mathbf{Q}}(i)_{k,m} = \tilde{q}_{km}^i = \frac{1}{2}E\{\tilde{w}_i[n,k]\tilde{w}_i^*[n,m]\}$ can be obtained from (17) such that

$$\tilde{q}_{km}^i = \begin{cases} \sum_{l=0}^{L} \sigma_{z_{i,l}}^2 p(k-l)p(m-l), & \text{if } 0 \le k-l \le L_p \\ & \text{and } 0 \le m-l \le L_p \\ 0 & \text{otherwise} \end{cases} \tag{25}$$

where $\sigma_{z_{i,l}}^2$ denote the variance of the noise sequences $z_{i,l}(k)$ of Figure 4. Letting

$$\mathbf{C}_{i,k} = [\mathbf{0}_{(i-1)(L+1)}, a_k, \cdots, a_{k-L}, \mathbf{0}_{(N_A-i)(L+1)}, \mathbf{0}_{N_A(\gamma-1)(L+1)}]$$

where $\mathbf{0}_D$ is zero row vector of length D, then the observation vector $\mathbf{y}[k]$ of (21) is defined as $\mathbf{y}[k] = [y_1[k], \cdots, y_{N_A}[k]]^T$, and $\mathbf{C}_k = [\mathbf{C}_{1,k}^T, \mathbf{C}_{2,k}^T, \cdots, \mathbf{C}_{N_A,k}^T]^T$ where $\mathbf{C}_k$ is of dimension $N_A \times \gamma(L+1)N_A$, and $\boldsymbol{\nu}[k] = [\nu_1[k], \cdots, \nu_{N_A}[k]]^T$ is the zero mean white Gaussian noise vector, with covariance matrix $\mathbf{R} = \sigma_\nu^2 I_{N_A}$.

For the system of (20,21) the Kalman Filter algorithm and the RLS algorithm directly follows and can be found in [2], [4]; however we must mention briefly that during the reception of the training sequence, the state space matrices are first estimated and used during the channel-state tracking phase. The estimations are justified as follows: Consider the state equation (20). Multiplying both sides by $\mathbf{x}^H[k]$ and taking expectation we get

$$2R_\mathbf{x}[1] = 2\mathbf{A}R_\mathbf{x}[0] + \mathbf{B}E\{\mathbf{W}[k+1]\mathbf{x}^H[k]\}.$$

Since $\mathbf{W}[k+1]$ is a uncorrelated with $\mathbf{x}[k]$ we get

$$\mathbf{A} = R_\mathbf{x}[1]R_\mathbf{x}^{-1}[0].$$

Similarly multiplying both sides of state equation by $\mathbf{x}^H[k+1]$ and taking expectation we get

$$2R_\mathbf{x}[0] = 2\mathbf{A}R_\mathbf{x}[1] + \mathbf{B}E\{\mathbf{W}[k+1]\mathbf{x}^H[k+1]\}.$$

Substituting (20), and using (24) we conclude

$$\mathbf{B}\mathbf{Q}\mathbf{B}^H = R_\mathbf{x}[0] - \mathbf{A}R_\mathbf{x}[1].$$

However the estimators of the autocorrelations will be used in the actual implementations of the algorithm.

V. Simulations of the Algorithm

After making the aforementioned extensions, the performance of RLS and Kalman channel state estimators coupled with PBP-MLSE [4] is demonstrated for QPSK symbols, with raised cosine pulse (truncated to a single symbol interval) being transmitted over the wireless channel with 3 taps (half-symbol spaced) with fractional powers 0.5, 0.3 and 0.2, with $N_a = 2$. Sampling rate of twice the symbol rate is assumed. A maximum Doppler shift of 83.33 Hz is observed under the conditions as in Section III. The system performance was evaluated with respect to *average bit-energy-to-noise ratio* γ_{ave}^b defined by

$$\gamma_{ave}^b = \frac{1}{N_A \log_2 M} \sum_{i=1}^{N_A} \frac{E\{|d_k|^2\} \sum_{k=0}^{L} E\{|h_i[\cdot,k]|^2\}}{2N_0}$$

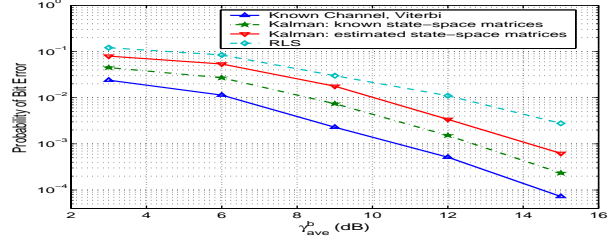MLSE-PBP algorithm with perfectly known channel states

Fig. 6: Bit error probability performance of the algorithm.

(at every sampling/time instant) has been provided as an optimal bound which is not practically possible. Then two different cases of Kalman channel state tracker has been provided as well: with and without known channel state matrices $(\mathbf{A}, \mathbf{B}\mathbf{Q}\mathbf{B}^H, \mathbf{R})$. For the unknown case those matrices were estimated during the training sequence phase.

References

[1] P. Bello, "Characterization of random time-variant linear channels", *IEEE Transactions on Communications*, vol. 11, pp. 360-393, December 1963.

[2] Q. Dai and E. Shwedyk, "Detection of Bandlimited Signals over Frequency Selective Rayleigh Fading Channels", *IEEE Transactions on Communications*, vol. 42, pp. 941-950, February/March/April 1994.

[3] W. C. Jakes Jr., *Microwave Mobile Communication*, New York: Wiley, 1974, p. 75.

[4] M. J. Omidi, S. Pasupathy and P. G. Gulak, "Joint Data and Channel Estimation for Rayleigh Fading Channels" *Wireless Personal Communications*, vol. 10, pp. 319-339, 1999.

[5] J. G. Proakis, *Digital Communications*, Third Edition, New York: McGraw-Hill, 1995.

[6] J. G. Proakis and D. G. Manolakis, *Digital Signal Processing: Principles, Algorithms, and Applications*, Third Edition, New Jersey: Prentice Hall, 1996.

[7] G. Stüber, *Principles of Mobile Communication*, Massachusetts: Kluwer Academic, 1996.